

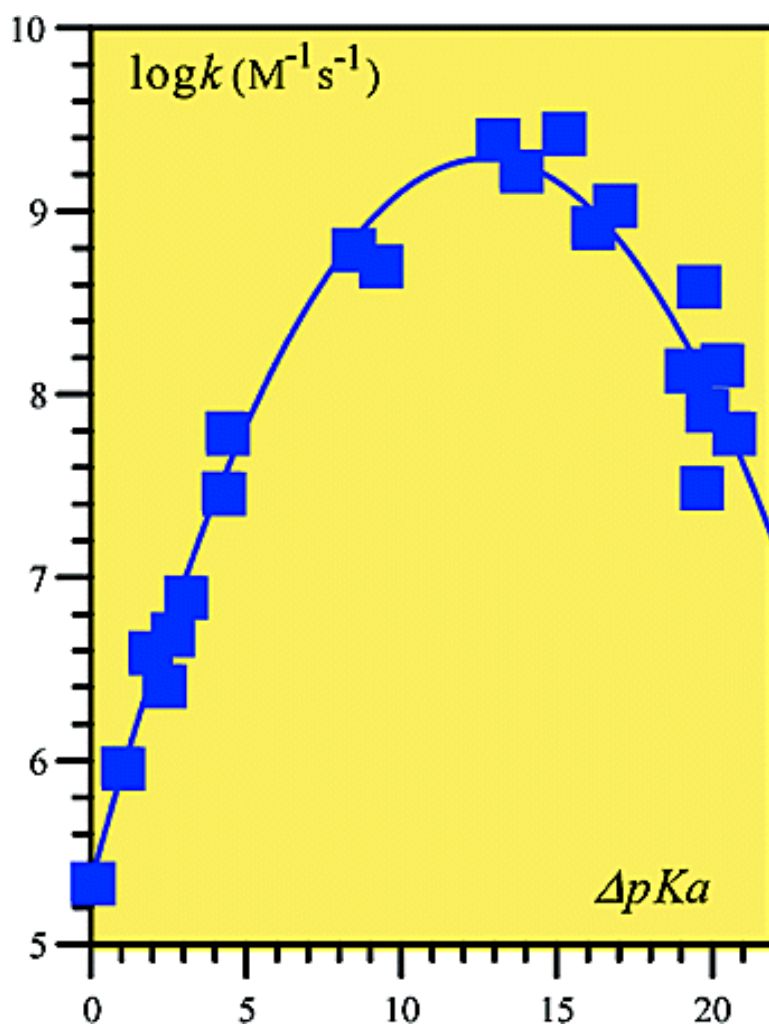
Article

Evidence for Inverted Region Behavior in Proton Transfer to Carbanions

Claude P. Andrieux, Jean Gamby, Philippe Hapiot, and Jean-Michel Savant

J. Am. Chem. Soc., **2003**, 125 (33), 10119-10124 • DOI: 10.1021/ja035268f • Publication Date (Web): 24 July 2003

Downloaded from <http://pubs.acs.org> on March 29, 2009



More About This Article

Additional resources and features associated with this article are available within the HTML version:



ACS Publications
 High quality. High impact.

- Supporting Information
- Links to the 4 articles that cite this article, as of the time of this article download
- Access to high resolution figures
- Links to articles and content related to this article
- Copyright permission to reproduce figures and/or text from this article

[View the Full Text HTML](#)



Evidence for Inverted Region Behavior in Proton Transfer to Carbanions

Claude P. Andrieux,^{1a} Jean Gamby,^{1a} Philippe Hapiot,^{1b} and Jean-Michel Savéant^{*1a}

Contribution from the Laboratoire d'Electrochimie Moléculaire, UMR 7591, Université de Paris 7, Denis Diderot, Case Courrier 7107, 2 place Jussieu, 75251 Paris Cedex 05, France and Laboratoire d'Electrochimie, Synthèse et Electrosynthèse Organiques, UMR 6510, Université de Rennes 1, Campus de Beaulieu, Bat. 10C, 35042 Rennes Cedex, France

Received March 21, 2003; E-mail: saveant@paris7.jussieu.fr

Abstract: The diphenylmethane–diphenylmethyl anion acid/base couple in *N,N*-dimethylformamide is taken as an example for investigating the dynamics of proton transfer at carbon in a system where the acid is not activated by an electron-withdrawing group or by removal of an electron. The laser flash electron photoinjection technique is applied to the determination of the rate constant for the protonation of diphenylmethyl anion by an extended series of acids that offers a range of driving forces encompassing over 1.2 eV. The plot of the rate constant versus the pK_a difference between diphenylmethane and the acids or of the activation free energy versus the standard free energy of the reaction exhibits clear “inverted region” behavior (by a factor of 80 in terms of rate constants). While such behaviors have been predicted and observed for outersphere electron-transfer reactions, previous evidence for proton-transfer reactions was scarce. Entropic factors, derived from an investigation of the temperature dependence of the experimental rate constants, are also discussed.

Introduction

So far, the investigation of protonation/deprotonation dynamics at carbon has been limited to molecules where acidity is boosted by introduction of an electron-withdrawing group^{2–4} or by removal of an electron.^{5–12} These restrictions can be removed by application of the laser flash electron photoinjection technique. In a preceding paper,¹³ we have described the procedures by which the protonation kinetics of carbanions not bearing electron-withdrawing substituents or not modified by removal of an electron can be measured by this technique under a wide variety of conditions, up to values close to the diffusion

limit. The purpose of the work depicted below was to apply the technique to the reaction of a diphenylmethyl anion with standard acids so as to cover a driving force range large enough

- (1) (a) Université de Paris 7. (b) Université de Rennes 1.
(2) (a) Fukuyama, M.; Flanagan, P. W. K.; Williams, F. T.; Frainer, L.; Miller, S. A.; Schechter, H. *J. Am. Chem. Soc.* **1970**, *92*, 4689. (b) Bordwell, F. G.; Boyle, W. J., Jr. *J. Am. Chem. Soc.* **1972**, *94*, 3907. (c) Bordwell, F. G.; Bartmess, J. E.; Hautala, J. A. *J. Org. Chem.* **1978**, *43*, 3107. (d) Kresge, A. J. *Can. J. Chem.* **1975**, *52*, 1897. (e) Keeffe, J. R.; Munderloh, N. H. *J. Chem. Soc., Chem. Commun.* **1974**, 17. (f) Keeffe, J. R.; Morey, J.; Palmer, C. A.; Lee, J. *J. Am. Chem. Soc.* **1979**, *101*, 1295. (g) Cox, B. G.; Gibson, A. *J. Chem. Soc., Chem. Commun.* **1974**, 638. (h) Wilson, J. C.; Källsson, I.; Saunders, W. H., Jr. *J. Am. Chem. Soc.* **1980**, *102*, 4780. (i) Amin, M.; Saunders, W. H., Jr. *J. Phys. Org. Chem.* **1993**, *6*, 393.
(3) (a) Bernasconi, C. F. *Acc. Chem. Res.* **1987**, *20*, 301. (b) Bernasconi, C. F.; Kliner, D. A. V.; Mullin, A. S.; Ni, J.-X. *J. Org. Chem.* **1988**, *53*, 3342. (c) Bernasconi, C. F. *Adv. Phys. Org. Chem.* **1992**, *27*, 119. (d) Albery, W. J.; Bernasconi, C. F.; Kresge, A. J. *J. Phys. Org. Chem.* **1988**, *1*, 29. (e) Bernasconi, C. F. *Acc. Chem. Res.* **1992**, *25*, 9. (f) Gandler, J. R.; Bernasconi, C. F. *J. Am. Chem. Soc.* **1992**, *114*, 631. (g) Bernasconi, C. F.; Wiersma, D.; Stronach, M. W. *J. Org. Chem.* **1993**, *58*, 217. (h) Bernasconi, C. F.; Ni, J.-X. *J. Org. Chem.* **1994**, *59*, 4910. (i) Bernasconi, C. F.; Panda, M.; Stronach, M. W. *J. Am. Chem. Soc.* **1995**, *117*, 9206. (j) Bernasconi, C. F.; Montanez, R. L. *J. Org. Chem.* **1997**, *62*, 8162. (k) Bernasconi, C. F.; Wenzel, P. J.; Keeffe, J. R.; Gronert, S. *J. Am. Chem. Soc.* **1997**, *119*, 4008. (l) Bernasconi, C. F.; Kittredge, K. W. *J. Org. Chem.* **1998**, *63*, 1994. (m) Bernasconi, C. F.; Ali, M.; Gunter, J. C. *J. Am. Chem. Soc.* **2003**, *125*, 151.
(4) (a) Farrell, P. G.; Fogel, P.; Chatrousse, A. P.; Lelièvre, J.; Terrier, F. *J. Chem. Soc., Perkin Trans. 2* **1985**, 51. (b) Fogel, P.; Farrell, P. G.; Lelièvre, J.; Chatrousse, A. P.; Terrier, F. *J. Chem. Soc., Perkin Trans. 2* **1985**, 711. (c) Terrier, F.; Lelièvre, J.; Chatrousse, A. P.; Farrell, P. G. *J. Chem. Soc., Perkin Trans. 2* **1985**, 1479. (d) Lelièvre, J.; Farrell, P. G.; Terrier, F. *J. Chem. Soc., Perkin Trans. 2* **1986**, 333. (e) Farrell, P. G.; Terrier, F.; Xie, H. Q.; Boubaker, T. *J. Org. Chem.* **1990**, *55*, 2546. (f) Terrier, F.; Xie, H. Q.; Farrell, P. G. *J. Org. Chem.* **1990**, *55*, 2610. (g) Terrier, F.; Xie, H. Q.; Lelièvre, J.; Boubaker, T.; Farrell, P. G. *J. Chem. Soc., Perkin Trans. 2* **1990**, 1899. (h) Terrier, F.; Croisat, D.; Chatrousse, A. P.; Ponet, M. J.; Hallé, J. C.; Jacob, G. *J. Org. Chem.* **1992**, *57*, 3684. (i) Terrier, F.; Lan, X.; Farrell, P. G.; Moskowitz, D. *J. Chem. Soc., Perkin Trans. 2* **1992**, 1259. (j) Terrier, F.; Boubaker, T.; Xia, L.; Farrell, P. G. *J. Org. Chem.* **1992**, *57*, 3924. (k) Moutiers, G.; El Fahid, B.; Collot, A.-G.; Terrier, F. *J. Chem. Soc., Perkin Trans. 2* **1996**, 49. (l) Moutiers, G.; Thuet, V.; Terrier, F. *J. Chem. Soc., Perkin Trans. 2* **1997**, 1479. (m) Moutiers, G.; Reignieux, A.; Terrier, F. *J. Chem. Soc., Perkin Trans. 2* **1998**, 2489.
(5) Sinha, A.; Bruce, T. C. *J. Am. Chem. Soc.* **1984**, *106*, 7291.
(6) (a) Tolbert, L. M.; Khanna, R. K. *J. Am. Chem. Soc.* **1987**, *109*, 3477. (b) Tolbert, L. M.; Khanna, R. K.; Popp, A. E.; Gelbaum, L.; Bettomley, L. A. *J. Am. Chem. Soc.* **1990**, *112*, 2373.
(7) (a) Fukuzumi, S.; Kondo, Y.; Tanaka, T. *J. Chem. Soc., Perkin Trans. 2* **1984**, 673. (b) Fukuzumi, S.; Tokuda, Y.; Kitano, T.; Okamoto, T.; Otera, J. *J. Am. Chem. Soc.* **1993**, *115*, 8960.
(8) (a) Schlesener, C. J.; Amatore, C.; Kochi, J. K. *J. Am. Chem. Soc.* **1984**, *106*, 7472. (b) Schlesener, C. J.; Amatore, C.; Kochi, J. K. *J. Phys. Chem.* **1986**, *90*, 3747. (c) Masnovi, J. M.; Sankaraman, S.; Kochi, J. K. *J. Am. Chem. Soc.* **1989**, *111*, 2263. (d) Sankaraman, S.; Perrier, S.; Kochi, J. K. *J. Am. Chem. Soc.* **1989**, *111*, 6448.
(9) (a) Reitstoen, B.; Parker, V. D. *J. Am. Chem. Soc.* **1990**, *112*, 4698. (b) Parker, V. D.; Chao, Y.; Reitstoen, B. *J. Am. Chem. Soc.* **1991**, *113*, 2336. (c) Parker, V. D.; Tilstet, M. *J. Am. Chem. Soc.* **1991**, *113*, 8778.
(10) (a) Hapiot, P.; Moiroux, J.; Savéant, J.-M. *J. Am. Chem. Soc.* **1990**, *112*, 1337. (b) Anne, A.; Hapiot, P.; Moiroux, J.; Neta, P.; Savéant, J.-M. *J. Phys. Chem.* **1991**, *95*, 2370. (c) Anne, A.; Hapiot, P.; Moiroux, J.; Neta, P.; Savéant, J.-M. *J. Am. Chem. Soc.* **1992**, *114*, 4694. (d) Anne, A.; Fraoua, S.; Hapiot, P.; Moiroux, J.; Savéant, J.-M. *J. Am. Chem. Soc.* **1995**, *117*, 7412. (e) Anne, A.; Fraoua, S.; Grass, V.; Hapiot, P.; Moiroux, J.; Savéant, J.-M. *J. Am. Chem. Soc.* **1998**, *120*, 2951.

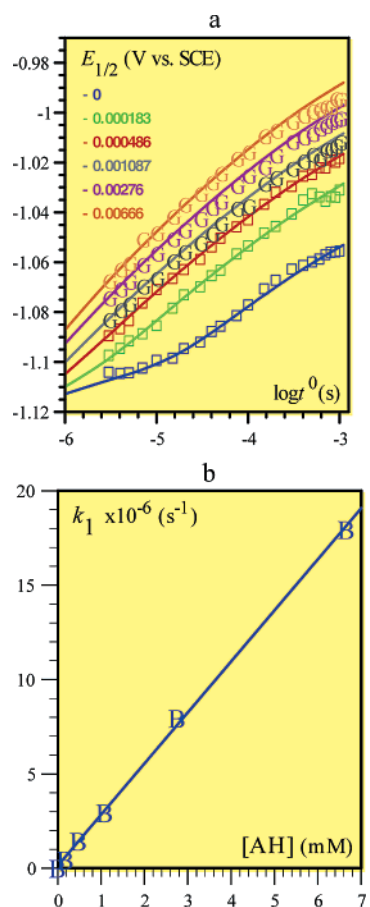
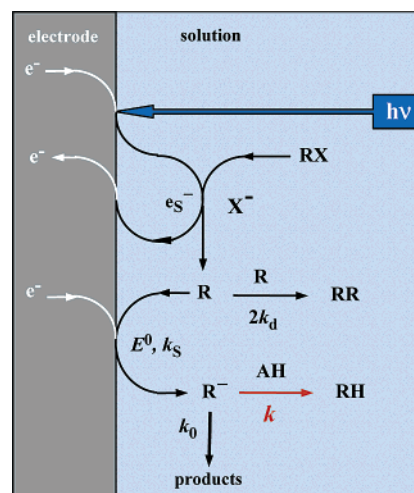


Figure 1. Reaction of diphenylmethyl anions with benzimidazole in DMF + 0.1 M Et_4NClO_4 at 22 °C. (a) Variations of the half-wave potential with measurement time for increasing concentrations of acid added (numbers, in M, of the same color as the data points); full lines, simulation for each acid concentration.¹³ (b) Pseudo-first-order rate constant as a function of benzimidazole concentration.

to make inverted region behavior, if any, appear. The solvent was *N,N*-dimethylformamide (DMF). While, such behaviors, exhibiting a decrease of the rate constant upon increasing the driving force of the reaction (decreasing the standard free energy of reaction), have been predicted¹⁴ and observed^{15,16} for outersphere electron-transfer reactions; previous evidence for proton-transfer reactions is scarce. It concerns¹⁷ the photochemically generated benzophenone/*N,N*-dimethylaniline radical ion pair and is rather modest in amplitude, ranging from 0 to a factor of 4 according to the nature of the solvent, the latter effect being observed in cyclohexane. The entropy and enthalpy of activation were derived from variation of the protonation rate constant with temperature. The discussion of the entropic factors will shed some light on the structure of the precursor and successor complexes.

- (11) (a) Bacciocchi, E.; Del Giacco, T.; Elisei, F. *J. Am. Chem. Soc.* **1993**, *115*, 12290. (b) Bacciocchi, E.; Bietti, M.; Putignani, L.; Steenken, S. *J. Am. Chem. Soc.* **1996**, *118*, 5952.
- (12) (a) Xu, W.; Mariano, P. S. *J. Am. Chem. Soc.* **1991**, *113*, 1431. (b) Xu, W.; Zhang, X.; Mariano, P. S. *J. Am. Chem. Soc.* **1991**, *113*, 8863.
- (13) Gamby, J.; Hapiot, P.; Savéant, J.-M., submitted.
- (14) Marcus, R. A. *J. Chem. Phys.* **1956**, *24*, 966.
- (15) (a) Miller, J. R.; Beitz, J. V. *J. Chem. Phys.* **1979**, *71*, 4579. (b) Miller, J. R.; Beitz, J. V.; Huddleston, R. K. *J. Am. Chem. Soc.* **1984**, *106*, 5057. (c) Miller, J. R.; Calcaterra, L. T.; Closs, G. L. *J. Am. Chem. Soc.* **1984**, *106*, 3047. (d) Miller, J. R.; Closs, G. L. *Science* **1988**, *240*, 4851.
- (16) (a) Farid, S. *Science* **1984**, *226*, 917. (b) Gould, I. R.; Farid, S. *Acc. Chem. Res.* **1996**, *29*, 522.
- (17) (a) Peters, K. S.; Cashin, A. *J. Phys. Chem. A* **2000**, *104*, 4833. (b) Peters, K. S.; Cashin, A.; Timbers, P. *J. Am. Chem. Soc.* **2000**, *122*, 107. (c) Peters, K. S.; Kim, G. *J. Phys. Chem. A* **2001**, *105*, 4177.

Scheme 1. Reactions Involved in an Electron Photoinjection Experiment Where the Diphenylmethyl Anion, R^- , Is Formed from the Reduction of the Diphenylmethyl Radical, R^\bullet , Generated from a Precursor, α -Chlorodiphenylmethane, by Means of Photoinjected Electrons and Reacted with an Acid, AH



Results

The experimental data consist, for each acid, and each concentration of the acid, of a series of photocurrent–dc potential sigmoid responses that are recorded as a function of the measurement time, t^0 .¹³ The half-wave potential, $E_{1/2}$, of these current–potential curves are plotted against $\log t^0$. For each acid, the experiments are repeated for 5–6 values of the acid concentration, leading to a set of data such as that shown in Figure 1a with the example where the acid is benzimidazole. The set of data pertaining to a given acid is then fitted, following previously described procedures leading to the set of full lines shown in Figure 1a,¹³ which corresponds to the various constants involved in Scheme 1 and yielding the values listed in Table 1. Among them is the protonation pseudo-first-order rate constant, which is then plotted against the acid concentration (Figure 1b), giving rise to a straight line with a slope that is the second-order protonation rate constant, k_{AH} , we are looking for. The fitting procedure is exemplified in Figure 1, while the corresponding data, fitting curves and k_1 – $[AH]$ plots are displayed in the Supporting Information for all experiments that have been performed. The log of the protonation rate constant thus obtained (Table 2) was then correlated with the difference of $\text{p}K_{\text{a}}$'s between each acid and diphenylmethane (Table 2). The $\text{p}K_{\text{a}}$'s were either taken directly from literature values or derived from $\text{p}K_{\text{a}}$'s in dimethylsulfoxide (DMSO) according to $\text{p}K_{\text{a,DMF}} = 1.5 + 0.96 \times \text{p}K_{\text{a,DMSO}}$.¹⁸ They are listed in the third column of Table 1. The $\text{p}K_{\text{a}}$ of diphenylmethane derived from its value in DMSO¹⁸ is 32.4. The plot of $\log k_{\text{AH}}$ against $\Delta \text{p}K_{\text{a}}$ is displayed in Figure 2.

- (18) (a) The $\text{p}K_{\text{a}}$'s are either taken directly from literature values or derived from $\text{p}K_{\text{a}}$'s in dimethyl sulfoxide (DMSO) according to $\text{p}K_{\text{a,DMF}} = 1.5 + 0.96 \times \text{p}K_{\text{a,DMSO}}$.^{18b} In the case of benzhydrol, histamine, 4-methoxyphenylacetic acid, 4,4,4-trifluorobutanol, 3,3,3-trifluoropropanol, and 1,1,1-trifluoro-2-propanol, the $\text{p}K_{\text{a}}$'s in DMSO were derived from the $\text{p}K_{\text{a}}$ in water according to a correlation established in each series. The $\text{p}K_{\text{a}}$ of diphenylmethane derived from its value in DMSO^{18d,e} is 32.4. (b) Maran, F.; Celadon, D.; Severin, G.; Vianello, E. *J. Am. Chem. Soc.* **1991**, *113*, 9320. (c) Bordwell, F. G. *Acc. Chem. Res.* **1988**, *21*, 456. (d) Bartmess, J. E.; Scott, J. A.; McIver, R. T., Jr. *J. Am. Chem. Soc.* **1979**, *101*, 6056. (e) Nielsen, M. F.; Hammerich, O.; Parker, V. D. *Acta Chem. Scand.* **1984**, *B38*, 809. (f) Lide, D. R. *HandBook of Chemistry and Physics*, Dissociation constants of organic Acids and Bases, 81st ed; 2000–2002; section 8–46. (g) http://scgc.epfl.ch/load/cours_chim/col_kj_2.pdf.

Table 1. Characteristic Constants Used in the Treatment of the $E_{1/2} - \log I^0$ Data^a

AH	compd no.	pK _a	temp (°C)	$\Gamma^0 \times 10^{13}$ (mol cm ⁻²)	$2k_d \sqrt{D} \times 10^{-14}$ (mol ⁻¹ cm ² s ^{-1/2})	$-E^\circ$ (V vs SCE)	$k_d/\sqrt{D} \times 10^{-3}$ (s ^{-1/2})	$k^\circ \times 10^{-4}$ (s ⁻¹)	$k_{AH} \times 10^{-8}$ (M ⁻¹ s ⁻¹)
tert-butanol	1	32.4	22	0.435	6.64	1.1035	2.21	6.79	0.002 21
			4.8	1.092	11.07	1.097	2.21	3.096	0.002 58
water	2	31.5	14.5	0.58	10.45	1.125	2.21	8.39	0.007 72
			22	0.308	5.06	1.102	2.21	6.42	0.010 96
			48	2	10.75	1.48	-	0.020 60	
			22	0.49	1.9	1.1085	2.21	8.23	0.038 80
2-propanol	3	30.6	22	0.99	6.64	1.1018	2.21	10.04	0.031 90
			40	0.93	9.48	1.0975	2.21	5.24	0.050 91
ethanol	4	30.1	22	0.85	6.64	1.1041	1.36	5.12	0.056 90
			2	1.36	2.53	1.0994	2.85	7.11	0.056 40
4,4,4-trifluoro-butanol	5	29.85	16	1.51	3.8	1.1053	1.36	10.54	0.057 23
			22	0.82	3.8	1.091	2.21	4.55	0.089 63
			34	1.53	5.37	1.0974	1.36	7.44	0.102 60
			2	1.42	5.53	1.1072	2.21	10.94	0.1490
methanol	6	29.4	18	1.46	6.64	1.0931	1.36	8.72	0.1884
			30	1.37	5.7	1.1033	0.95	9.37	0.2204
			22	0.95	6.64	1.099	2.21	9.10	0.6405
benzhydryl	7	28.2	22	0.7	9.48	1.087	1.74	12.7	4.79
			42	0.69	18.97	1.088	1.42	18.1	4.48
3,3,3-trifluoropropanol	8	28.05	52.5	0.82	18.97	1.087	1.48	12.4	4.76
			22	0.68	11.07	1.1087	2.21	6.034	5.135
			21.5	0.94	7.9	1.0989	2.21	0.75	23.92
2,2,2-trifluoro ethanol	9	24	31	0.97	14.23	1.084	1.9	0.314	27.7
			41.5	0.78	12.64	1.087	1.26	8.17	24.9
			52.5	0.76	25.2	1.086	1.6	12.81	24.48
			22	0.52	5.7	1.0946	2.21	1.458	16.72
1,1,1-trifluoro-2-propanol	10	23.15	22	0.64	5.37	1.1024	1.64	14.04	27.04
			22	0.94	7.9	1.0989	2.21	0.75	23.92
imidazole	11	19.35	31	0.97	14.23	1.084	1.9	0.314	27.7
			41.5	0.78	12.64	1.087	1.26	8.17	24.9
			52.5	0.76	25.2	1.086	1.6	12.81	24.48
			22	0.52	5.7	1.0946	2.21	1.458	16.72
histamine	12	18.6	22	0.52	5.7	1.0946	2.21	1.458	16.72
benzimidazole	13	17.25	22	0.64	5.37	1.1024	1.64	14.04	27.04
benzyl mercaptan	14	16.3	-5	1.42	1.58	1.093	1.36	41.6	7.462
			16	1.6	3.16	1.36	1.36	8.365	
			40	1.9	3.8	1.36	8.45	9.346	
			50.5	2	5.37	1.36	11.437		
triazole	15	15.6	22	0.68	5.37	1.099	2.21	14.78	10.97
acetic acid	16	13.3	-15.0	0.61	2.8	1.1006	2.8	15.2	0.612
			1.0	0.61	4.7	1.1052	2.8	10.7	0.916
			16.0	0.55	10.4	1.1053	1.6	7.95	1.349
			44.0	0.47	21.5	1.0984	1.6	11.5	2.0047
			58.0	0.49	37.8	1.1008	1.14	12.6	2.3108
			22	0.735	3.47	1.0917	2.21	7.68	3.974
4-methoxy phenylacetic acid	17	12.9	22	0.805	5.06	1.12	1.36	6.33	0.318
phenylacetic acid	18	12.8	22	0.75	7.9	1.1016	2.21	5.65	0.836
			19	0.65	14.23	1.0935	2.21	15.25	1.424
benzoic acid	19	12.15	26	1.31	6.32	1.111	2.21	6.1	2.120
			35	0.58	15.8	1.0932	1.97	9.85	2.944
			45.5	0.705	15.8	1.1014	2.21	12.9	3.342
			22	0.85	6.64	1.12	2.1	16.48	0.67
perfluoro-tert-butanol	21	11.8	22	0.85	6.64	1.12	2.1	16.48	0.67

^a Γ^0 : initial surface concentration of radicals. D : diffusion coefficient. k_d : dimerization rate constant. E° : standard potential. k° : rate constant of the reaction of the carbanion with the reaction medium. k_{AH} : protonation rate constant.

The next step was carrying out an investigation of the temperature dependence of the protonation rate constant. Since gathering the experimental results and performing the simulation for extracting the protonation rate constants are rather tedious, we restricted the investigation to a smaller list of acids, selecting representatives (Table 3) of each of the families in the global list of 21 acids (Table 2). Detailed results and simulation are given in the Supporting Information. The Arrhenius plots are shown in Figure 3 (results in Table 3).

Discussion

The protonation rate constant starts to increase with the difference in pK_a (Figure 2), passes through a maximum, and then decreases upon further increases of ΔpK_a , thus exhibiting clear-cut “inverted region” behavior. There are very few reports, actually only one¹⁷, of inverted region behavior in proton transfer reactions. It concerns the photochemically generated benzophe-

none/*N,N*-dimethylaniline radical ion pair, thus involving a carbon acid. Its magnitude varies with the solvent but remains very modest in amplitude, being at best equal to a factor of 4 in terms of rate constants (in the least polar solvent, cyclohexane). In the present case, the effect is much larger, the rate constant varying by a factor of 80 upon passing from the high driving force lower point to the maximum of the rate constant.

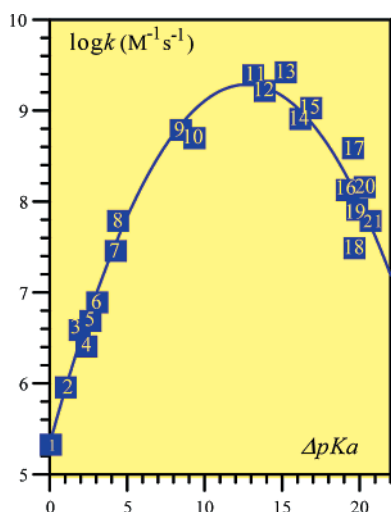
The data points in the $\log k_{AH}$ versus ΔpK_a activation-driving force plot of Figure 2 may be fitted with the following parabola.

$$\log k_{AH} = 5.33 + 0.62 \times \Delta pK_a - 0.024 \times (\Delta pK_a)^2$$

which may be converted into a quadratic correlation between the free energy of activation, ΔG^\ddagger , and the standard free energy of the reaction, ΔG° . From a theoretical standpoint, models have been designed that lead to quadratic relationships between free energy of activation and standard free energy of the reaction,

Table 2. Free Energy of Activation and Standard Free Energy of the Reaction of Diphenylmethyl Carbanion with Acids

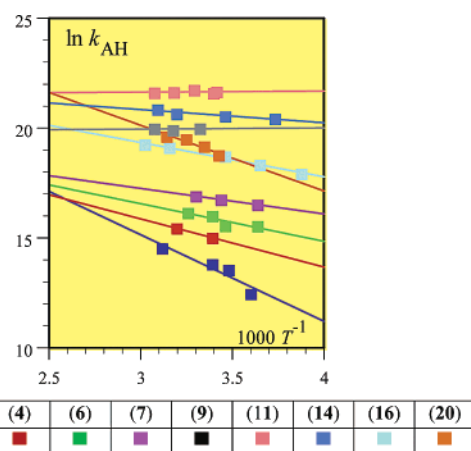
AH	compd no.	pK _a (DMF)	ΔpK _a	log k _{AH} (M ⁻¹ s ⁻¹)	ΔG [‡] (eV)	ΔG [°] (eV)
<i>tert</i> -butanol	1	32.4 ^{18c,e}	0.0	5.3	0.000	0.241
water	2	31.5 ^{18a,c,d}	1.0	5.6	-0.056	0.204
2-propanol	3	30.6 ^{18c}	1.9	6.6	-0.109	0.167
ethanol	4	30.1 ^{18e}	2.3	6.4	-0.135	0.177
4,4,4-trifluorobutanol	5	29.85 ^{18a,g}	2.6	6.7	-0.150	0.161
methanol	6	29.4 ^{18c,e}	3.0	6.9	-0.176	0.149
benzhydrol	7	28.2 ^{18a,d}	4.2	7.5	-0.246	0.116
3,3,3-trifluoropropanol	8	28.05 ^{18a,g}	4.3	7.8	-0.254	0.097
2,2,2-trifluoroethanol	9	24 ^{18c}	8.4	8.8	-0.491	0.038
1,1,1-trifluoro-2-propanol	10	23.15 ^{18a,g}	9.3	8.7	-0.543	0.043
imidazole	11	19.35 ^{18c}	13.1	9.4	-0.764	0.003
histamine	12	18.6 ^{18a,f}	13.8	9.2	-0.808	0.013
benzimidazole	13	17.25 ^{18c}	15.2	9.4	-0.888	0.001
benzyl mercaptan	14	16.3 ^{18c}	16.1	8.9	-0.943	0.031
triazole	15	15.6 ^{18c}	16.8	9.0	-0.984	0.024
acetic acid	16	13.3 ^{18b,c}	19.1	8.1	-1.119	0.077
benzotriazole	17	12.9 ^{18c}	19.5	8.6	-1.142	0.050
4-methoxyphenylacetic	18	12.8 ^{18a,f}	19.6	7.5	-1.148	0.090
phenylacetic	19	12.65 ^{18b}	19.8	7.9	-1.158	0.089
benzoic acid	20	12.15 ^{18b,c}	20.3	8.2	-1.186	0.075
perfluoro- <i>tert</i> -butanol	21	11.8 ^{18c}	20.6	7.8	-1.208	0.114

**Figure 2.** Reaction of diphenylmethyl anions with acids in DMF + 0.1 M Et₄NClO₄ at 22 °C. Variation of the protonation rate constant with the driving force measured by ΔpK_a.**Table 3.** Reaction of Diphenylmethyl Carbanion with Acids: Slope and Intercept of the Arrhenius Plots and Activation Entropy and Enthalpy

AH	compd no.	slope	intercept	ΔH [‡] (eV)	ΔS [‡] (meV/K)
water	2	3941	26.9	0.340	-0.217
ethanol	4	2195	22.5	0.189	-0.601
methanol	6	1712	21.7	0.147	-0.666
benzhydrol	7	1161	20.7	0.100	-0.666
2,2,2-trifluoroethanol	9	53.77	19.2	0.005	-0.882
imidazole	11	-45.39	21.5	-0.004	-0.683
benzyl mercaptan	14	598.4	22.6	0.052	-0.585
acetic acid	16	1562	24.0	0.135	-0.465
benzoic acid	20	2990	29.16	0.258	-0.028

formally similar to the relationships applicable to outersphere electron-transfer reactions.¹⁹ To test this type of relationship, the log k_{AH} - ΔpK_a plot is thus converted into a ΔG[‡] - ΔG[°]

(19) (a) See ref 19b,c and references therein. (b) Kiefer, P. M.; Hynes, J. T. *J. Phys. Chem. A* **2002**, *106*, 1834. (b) Kiefer, P. M.; Hynes, J. T. *J. Phys. Chem. A* **2002**, *106*, 1850.

**Figure 3.** Reaction of diphenylmethyl anions with acids in DMF + 0.1 M Et₄NClO₄. Arrhenius plots.

plot (Table 2), according to

$$\Delta G^{\circ}(\text{eV}) = \frac{RT}{F} \Delta \text{p}K_{\text{a}}$$

$$\Delta G^{\ddagger}(\text{eV}) = \frac{RT}{F} \ln \frac{k_{\text{max}}}{k_{\text{AH}}} \quad (1)$$

In this conversion, the possibility of a partial diffusion control of the reaction has been neglected, since the maximal value of k_{AH}, 2.7 × 10⁹ M⁻¹ s⁻¹, is sufficiently below the diffusion limit, 10¹⁰ M⁻¹ s⁻¹. We have also adjusted the parameter k_{max} so that the reaction is barrierless at the apex of the ΔG[‡] - ΔG[°] curve. This would require k_{max} = 2.7 × 10⁹ M⁻¹ s⁻¹. In other words, we consider that bringing the reactant together from infinite separation, before proton transfer takes place, requires a work term, w_R = 0.195 eV, for the value of ΔG[°] corresponding to the apex of the parabola. The value of k_{max} may also result, at least partly, from a lack of adiabaticity of the proton-transfer reaction. The ensuing ΔG[‡] - ΔG[°] plot is displayed in Figure 4.

The simplest approach is then to test the validity of the classical quadratic eq 2, in which λ stands for the total reorganization energy attending proton transfer:

$$\Delta G^{\ddagger} = \frac{\lambda}{4} \left(1 + \frac{\Delta G^{\circ}}{\lambda} \right)^2 = \frac{\lambda}{4} + \frac{\Delta G^{\circ}}{2} + \frac{\Delta G^{\circ 2}}{4\lambda} \quad (2)$$

In fact, the best quadratic fitting (blue curve in Figure 4)

$$\Delta G^{\ddagger} = 0.24 + 0.62\Delta G^{\circ} + 0.42\Delta G^{\circ 2}$$

does not exactly match eq 2 in the sense that the coefficient of the ΔG[°] term is significantly different from 0.5, the classical value of the symmetry factor at zero driving force. This observation points to a lack of symmetry in the response of the reorganization factors (solvent + intramolecular movements) to the departure from equilibrium in the initial and final states. We may therefore test another relationship deriving from the intersection of the two following potential energy curves, involving the reorganization coordinate, X, with two different values of the reorganization factor λ_R and λ_P, for the reactant and product systems, respectively:

$$G_{\text{R}} = \lambda_{\text{R}}X^2, G_{\text{P}} = \Delta G^{\circ} + \lambda_{\text{P}}(1 - X)^2$$

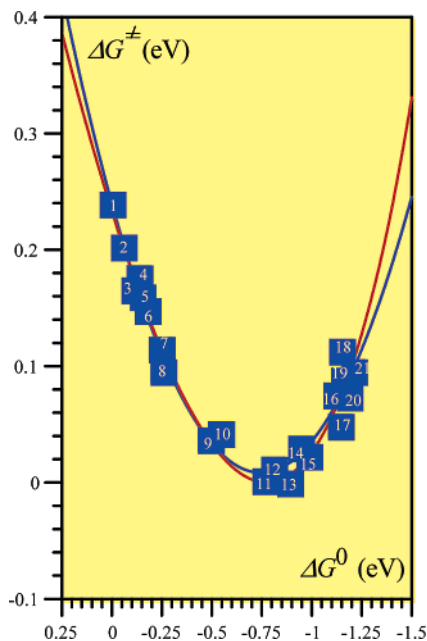


Figure 4. Reaction of diphenylmethyl anions with acids in DMF + 0.1 M Et₄NClO₄ at 22 °C. Variation of the activation free energy with the standard free energy of the reaction. Blue curve: fitting according to eq 2. Red curve: fitting according to eq 3.

At the transition state,

$$X^{\ddagger} = \frac{-1 + \sqrt{1 + \frac{\lambda_R - \lambda_P}{\lambda_P} \left(1 + \frac{\Delta G^\circ}{\lambda_P}\right)}}{\frac{\lambda_R - \lambda_P}{\lambda_P}} \quad (3)$$

$$\Delta G^{\ddagger} = \lambda_R X^{\ddagger 2}$$

The fit of the data points with eq 3 (red curve in Figure 4) is excellent, even better than with eq 1, leading to $\lambda_R = 1.15$ eV and $\lambda_P = 0.77$ eV.

The activation entropies derived from the intercept of the Arrhenius plot, taking into account the definition of ΔG^{\ddagger} in eq 1 (Table 3), are displayed as a function of the standard free energy of the reaction in Figure 5. Rather than the entropy itself, we have plotted its product by 295.16 K so as to get an idea of the magnitude of the entropic effect in terms of energy. It is remarkable that it starts to decrease with ΔG° and then passes through a minimum, in the vicinity of the $\Delta G^{\ddagger} - \Delta G^\circ$ minimum, before increasing upon continuing to decrease ΔG° .

These observations may be rationalized as follows. We may divide the entropy of activation into two contributions. One involves the change in solvation from the initial state to the transition state. It is a positive contribution since the charge is more delocalized in the latter state than in the former. As ΔG° decreases, the symmetry factor decreases implying that the transition state resembles more and more the initial state, making the solvation contribution less and less important. The other contribution pertains to the nuclear configuration of the reacting system. It is negative in the sense that the transition state is more ordered than the initial state. Upon entering the inversion region, the reaction coordinate goes in the reverse direction making the transition state less ordered than the initial state. The combination of the variation of the two contributions with

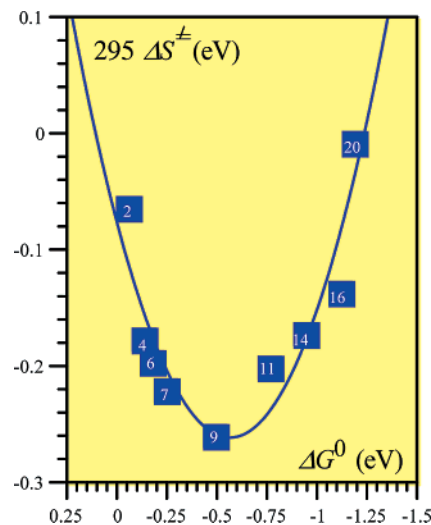


Figure 5. Reaction of diphenylmethyl anions with acids in DMF + 0.1 M Et₄NClO₄. Variation of the activation entropy with the standard free energy of the reaction.

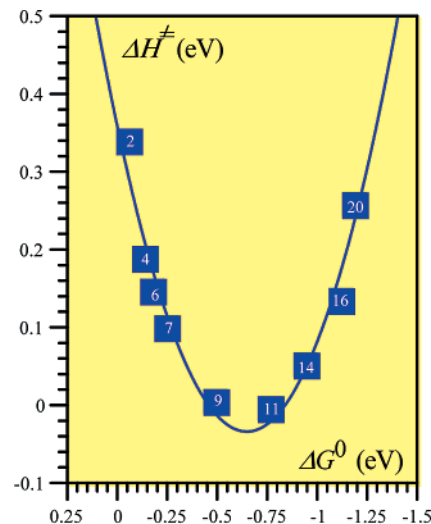


Figure 6. Reaction of diphenylmethyl anions with acids in DMF + 0.1 M Et₄NClO₄. Variation of the activation enthalpy with the standard free energy of the reaction.

the driving force results in a decrease followed by an increase of ΔS^{\ddagger} upon decreasing ΔG° .

The enthalpy of activation, ΔH^{\ddagger} , may finally be derived from the Arrhenius slopes (Table 3). The $\Delta H^{\ddagger} - \Delta G^\circ$ plot (Figure 6) exhibits even more striking inverted region behavior than the free energy plot, spanning over more than 0.35 eV.

Concluding Remarks

Taking the diphenylmethane/diphenylmethyl anion couple as an example of an acid/base system where the acid is not activated by an electron-withdrawing group or by removal of an electron, we may summarize the conclusions of the present study and the preceding article¹³ in the series as follows. The proton transfer reaction is intrinsically slow, exhibits an important isotope kinetic effect, and shows clear evidence of inverted region behavior. The activation–driving force plots may be fitted with the relationship deriving from the intersection of two potential energy curves in which the reorganization factor pertaining to the reactant and product systems is different. The average value of the reorganization energy, of the order of 1

eV, points to a significant contribution of internal reorganization in addition to solvent reorganization.

Supporting Information Available: Fitting of the half-wave potential versus measurement time curves obtained for increas-

ing values of the acid added, leading to the parameter values listed in Table 1, and curves of pseudo-first-rate constants as a function of acid concentration

JA035268F